

Characterization of silver nanoparticles by green synthesis method using *Pedalium murex* leaf extract and their antibacterial activity

K. Anandalakshmi¹ · J. Venugopal² · V. Ramasamy²

Received: 27 February 2015 / Accepted: 12 April 2015 / Published online: 16 May 2015
© The Author(s) 2015. This article is published with open access at Springerlink.com

Abstract In this paper, an aqueous extract of fresh leaves of *Pedalium murex* was used for the synthesis of silver (Ag) nanoparticles. Different biological methods are gaining recognition for the production of silver nanoparticles (AgNPs) due to their multiple applications. The use of plants in the green synthesis of nanoparticles emerges as a cost-effective and eco-friendly approach. Characterization of nanoparticles was done using different methods, which include; ultraviolet–visible spectroscopy (UV–Vis), Fourier transform infrared (FTIR), powder X-ray diffraction (XRD), field emission scanning electron microscope (FE-SEM), energy dispersive X-ray analysis (EDAX), fluorescence emission spectroscopy, transmission electron microscope (TEM), dynamic light scattering (DLS), zeta potential and antibacterial activity. UV–visible spectrum of the aqueous medium containing silver nanoparticles showed absorption peak at around 430 nm. Fourier transform infrared spectra had shown that the biomolecule compounds were responsible for the reduction and capping material of silver nanoparticles. XRD study showed the particles to be crystalline in nature, with a face-centered cubic (fcc) structure. The size and stability were detected using DLS and zeta potential analysis. The antibacterial activity of AgNPs against generally found bacteria was

assessed to find their potential use in silver-containing antibacterial product.

Keywords Green synthesis · SNPs · Leaf extract · XRD · TEM · Antibacterial activity

Introduction

Nano-biotechnology has emerged as an important division of nanotechnology. One of the important aspects in the field of nanotechnology is the development of a more consistent process for the synthesis of nanomaterials more than a range of size (with good monodispersity) and chemical composition (Rai et al. 2011). Noble metal nanoparticles have been gaining a lot of significance in the past few years due to their applicability in the field of physics, chemistry, medicine, biology and material science (Yokohama and Welchons 2007). Metal nanoparticles have a high specific surface area and surface atoms, because of their outstanding physicochemical characteristics, including optical, catalytic, electronic, magnetic and antibacterial properties. Synthesis of metal nanoparticles is enormous due to their potential applicability in different areas such as electronics, chemistry, energy, and medicine development (Saxena et al. 2012). Metal nanoparticles, particularly noble metals, have been studied mainly because of their strong optical absorption in the visible region caused by the group excitation of the free electron gas (Mohamed et al. 2000). The silver nanoparticles have a large area of interest as they have a large number of applications: nonlinear optics, spectrally selective coating for solar energy absorption, biolabeling, intercalation materials for electrical batteries as optical receptors, catalyst in chemical reactions, antibacterial

✉ K. Anandalakshmi
anandhi8888@gmail.com

¹ Department of Engineering Physics, Annamalai University, Annamalainagar 608 002, Tamil Nadu, India

² Department of Physics, Annamalai University, Annamalainagar 608 002, Tamil Nadu, India

materials, chemically stable materials and good electrical conductors (Zargar et al. 2014; Sharma et al. 2009). They are ahead of time the interest of researchers for their novel method for synthesis of silver nanoparticles. Silver is well known for possessing an inhibitory result toward many bacterial strains and microorganisms commonly present in medical and industrial processes (Jiang et al. 2004). The general method of synthesizing silver nanoparticles in chemical reduction is as colloidal dispersions in water or organic solvents (Sharma et al. 2009). The green synthesis method utilizes nontoxic chemicals, eco-friendly solvent and renewable materials (Raveendran et al. 2003). In the medical field, silver and silver nanoparticles have broad applications, especially in skin ointments and creams to avoid infection of burns and open wounds (Duran et al. 2005). Ag nanoparticles have been synthesised by different physical and chemical approaches viz., chemical reduction, microemulsion/reverse micelles, electrochemical reduction and photochemical reduction. Many biological approaches of green synthesis have been reported till date using plant leaf extracts from *Alternanthera sessilis* (Niraimathi et al. 2013), *Morinda citrifolia* (Sathishkumar et al. 2012), *Mukia scabrella* (Prabakar et al. 2013), *Iresine herbstii* (Dipankar and Murugan 2012), *Tribulus terrestris* (Gopinath et al. 2012), *Azadirachta indica* (Khan et al. 2012), *Cycas circinalis*, *Ficus amplissima*, *Commelina benghalensis*, *Lippia nodiflora* (Johnson and Prabu 2015), *Ocimum sanctum* (Garima Singhal et al. 2011) and *Aloe vera* (Medda et al. 2014). *Petalium murex* (*P. murex*) is a member of the sesame family, Pedaliaceae. It is found in different parts of the world such as tropical Africa, Sri Lanka, India, Mexico and Pakistan (Rajashekar et al. 2012). It has been usually used for the treatment of puerperal diseases, as digestive tonics and in the treatment of ulcers, fevers, wounds, other ailments and general debility. Naturally, we were tempted to verify the wisdom of the local community in using these plants as herbal drugs. The plant is sweet, cooling, mucilaginous, diuretic and anti-inflammatory and used to treat digestive, carminative, tonic and puerperal affections, spermatorrhea, spasmodic affections, amenorrhoea, dysmenorrhoea, vitiated conditions of pita, inflammation and general debility. A decoction of leaves is given in cases of gonorrhoea, while that root is said to be antibilious. The whole plant of *P. murex* is used as a remedy to cure stomachache, headache, diarrhea, dysentery, cough and cold, intestinal infections, etc. So far, there has been no report on the green synthesis of nanoparticles using *Petalium murex* leaves extract. The presently investigate the synthesis of silver nanoparticles from *Petalium murex* extract and ascertain their characterization.

Materials and methods

Plants and chemicals

AR-grade silver nitrate (AgNO_3) was purchased from Sigma-Aldrich Chemicals and fresh *Petalium murex* leaves were collected from the Agricultural Department, Annamalai University, Tamil Nadu, India. Double-distilled water was used for the experiments.

Preparation of the extract

Fresh leaf *Petalium murex* extract was used for the reduction of Ag^+ ions to Ag^0 . The plant leaf extract solutions were prepared by taking leaves and drying at room temperature. These leaves were ground into a fine powder in a 500 ml Erlenmeyer flask. 5 g of fine powder along with 100 ml of distilled water was boiled for 10 min before decanting. Further, the extract was filtered with Whatman no.1 filter paper, stored at 4 °C and used for further experiments.

Synthesis of silver nanoparticles

An aqueous solution (0.01 mM) of silver nitrate (AgNO_3) and various concentrations of leaf extract from 1 to 5 ml were prepared separately. Each concentration of the leaf extract was added to 10 ml of 0.01 mM AgNO_3 prepared solution. After 20 min, the color of the solution (leaf extract + Ag^+) changed from light yellow to dark brown, indicating the formation of AgNPs. The resulting colloidal solution of silver was analyzed using UV–Vis spectrophotometer.

Microorganisms

The evaluation of antibacterial activity was carried out using seven different stains. These following microorganisms were used: *Bacillus subtilis*, *Staphylococcus aureus*, *Escherichia coli*, *Micrococcus flavus*, *Pseudomonas aeruginosa*, *Klebsiella pneumoniae* and *Bacillus pumilus*. These microorganisms were collected from the National Chemical Laboratory, Pune, India. The microbial cultures were maintained by the Department of Pharmacy, Annamalai University, Annamalai Nagar, Tamil Nadu, India.

Characterization techniques

UV–Vis spectroscopy is the most important technique and the simplest way to confirm the formation of nanoparticles. The absorbance spectrum of the colloidal sample was

obtained in the range of 200–800 nm, using a UV–Vis spectrometer Shimadzu-UV 1800 with distilled water as a reference. FTIR analysis was performed to classify the biomolecules in *Pedaliium murex* which were responsible for reduction of the metals and for the stabilization of nanoparticles. The functional group responsible for the silver nanoparticles was also analyzed using FTIR RX1-Perkin Elmer in the wavelength range 4000–400 cm^{-1} . The emission spectra were recorded using an LF-45 fluorescence spectrophotometer (Perkin Elmer). X-ray diffraction (XRD) analysis was conducted by XPERT-PRO using monochromatic Cu α radiation ($\lambda = 1.5406 \text{ \AA}$) operated at 40 kV and 30 mA at a 2θ angle pattern. The scanning was done in the region of 20° – 80° . The images obtained were compared with the Joint Committee on Powder Diffraction Standards (JCPDS) library to account for the crystalline structure. The morphology and shape of the silver nanoparticles were examined using field emission electron microscopy SUPRA55 (CARL ZEISS, Germany). EDAX analysis of silver nanoparticles was performed on a SUPRA55 (CARL ZEISS, Germany) using FESEM equipped with an EDAX attachment. TEM analysis was performed to determine the morphology, size and shape of the silver nanoparticles. TEM measurements were done by HITACHI H-800, operating at 200 kV. The TEM grid was prepared by placing a drop of the bio-reduced diluted solution on a carbon-coated copper grid and later drying it under a lamp. The size distribution and stability of AgNPs, DLS and zeta potential measurements were carried out using Malvern instruments.

Antibacterial activity

Antibacterial activity of the synthesized AgNPs was studied by the standard disc diffusion method. The overnight-grown bacterial suspensions of *Escherichia coli* (ATCC 8739), *Klebsiella pneumoniae* (ATCC 10031), *Micrococcus flavus* (ATCC 25619), *Pseudomonas aeruginosa* (ATCC 25619), *Bacillus subtilis* (ATCC 6633), *Bacillus pumilus* (ATCC 12228) and *Staphylococcus aureus* (ATCC 29737) were standardized using McFarland standard. Whatman filter paper (no: 1) discs of 5 mm diameter were used. The dilutions of biosynthesized AgNPs varying from 5, 10 and 15 $\mu\text{l/ml}$ were prepared with twofold symmetry. 5 g of solidified agar was added with 50 ml of distilled water and sterilized. This mixture was poured equally into seven Petri plates and seven organisms were plated in them. The organisms to be tested were inoculated in four discs (5 mm diameter) dipped in different dilutions of AgNPs (5, 10 and 15 $\mu\text{l/ml}$) solutions, and another disc was dipped in 2 mg/ml of antibiotic ofloxacin. Each Petri plate was loaded with these four discs. The plates containing the bacterial and AgNPs were incubated at 37°C and then

examined for confirmation, the appearance of a clear area around the disc. The diameter of such zones of inhibition was measured using a meter ruler, and the mean value for each organism was recorded and expressed in millimeters.

Results and discussion

UV–Vis spectral analysis

Figure 1 shows the leaves of the *Pedaliium murex* plant. Figure 2 shows the AgNO_3 solution before and after adding the leaf extract. The UV–visible absorption spectra of the Ag nanoparticles with different concentrations of *Pedaliium murex* leaf extract of 1, 2, 3, 4 and 5 ml are recorded and shown in Fig. 3. The formation of the AgNPs during the reduction process is indicated by change in the color of the reaction solution from colorless to dark brown which can be visually observed (Fig. 2). Metal nanoparticles have free electrons, which yield a surface plasmon resonance (SPR) absorption band, due to the mutual vibration of electrons of metal nanoparticles in resonance with light wave. The appearances of the peaks show the characteristics of surface plasmon resonance of silver nanoparticles.

The absorption spectra exhibit a gradual decrease of the absorbance, accompanied by a shift in the wavelength from 430 to 424 nm. A decrease in the FWHM value is also observed from Fig. 3. The increases in the intensity of the plasmon bands indicate the decrease in the band width



Fig. 1 Photograph of *Pedaliium murex* leaf



Fig. 2 Photograph of **a** AgNO_3 , and **b** synthesised silver nanoparticles

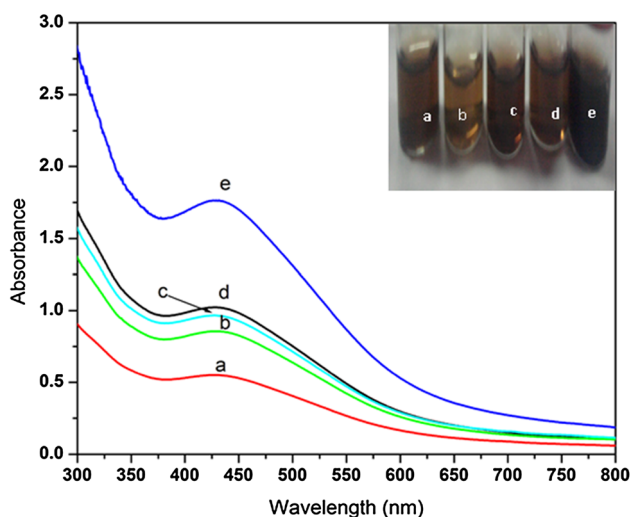


Fig. 3 UV–Vis spectra of synthesized AgNPs at different concentrations

(Zhang et al. 2006). The UV–Vis spectrum shows the important role of AgNO_3 and the presence of ingredients in the leaves for the formation of silver nanoparticles. The increase in the concentration of the leaf extract will also increase the absorbance intensity. It is also observed that the surface plasmon peak that occurs at 424 nm is slowly shifted toward lower wavelength at high concentrations. This shift may be due to blue shift and depends on the particle size and shape (Kelly et al. 2003; Lee and El-sayed 2006). According to Njagi et al. (2011), this band corresponds to the absorption by colloidal silver nanoparticles in the region (400–450 nm) due to the excitation of surface

plasmon vibration. So the high-concentration sample is used for further analysis. A high concentration of *Petalium murex* leaf extract increases the number of biocompounds required to reduce Ag^+ to Ag^0 .

Fluorescence

The PL of the synthesized bio-inspired AgNPs by *Petalium murex* leaf extract is also studied via fluorescence emission spectroscopy. Photoluminescence (PL) spectrum is one of the methods to estimate the optical property of silver nanoparticles as photonic materials. The colloidal silver nanoparticles are dispersed in water and the PL emission spectra are recorded for the excitation wavelength at 420 nm. A broad emission is obtained at 478 nm (Fig. 4). The intensity of fluorescence emission peak is gradually increased up to 478 nm, after which it is slowly decreased up to 650 nm. Earlier, a characteristic fluorescence peak of AgNPs in the water phase at 465 nm was reported (Jiang et al. 2005). Vigneshwaran et al. (2006) reported an emission peak of AgNPs produced from soluble starch at 553 nm. When compared with the value of AgNPs in the water phase (465 nm), the present peak is redshifted.

FTIR analysis of AgNPs

FTIR measurements were carried out to identify the possible biomolecules in the *Petalium murex* extract. FTIR spectra of dried aqueous extract and synthesised AgNPs are shown in Fig. 5. The phytochemical analysis of *Petalium murex* reveals the presence of flavonoids, alkaloids, steroids, rosins, saponins and proteins (Rajashekar et al. 2012; Patel et al. 2011). In leaf extract, the peaks are observed at 445, 617, 1075, 1287, 1421, 1602, 3157 and

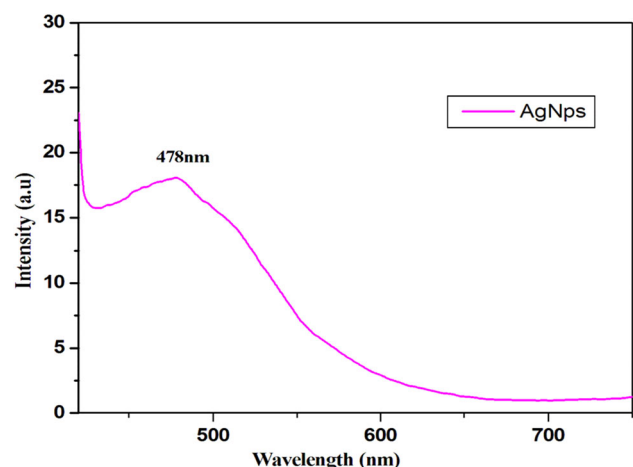


Fig. 4 Fluorescence emission spectra where $\lambda_{\text{ex}} = 430$ nm of AgNPs synthesized in *Petalium murex* leaf extract

3785 cm^{-1} , respectively. After reaction with AgNO_3 , the peaks are shifted to a higher wave number side, such as 456, 614, 1074, 1382, 1592, 3158 and 3881 cm^{-1} . The peak at 445 cm^{-1} of the extract is shifted toward a higher wave number side at 456 cm^{-1} due to the O–Si–O network and ring opening vibration. The band observed at 617 cm^{-1} is shifted to the lower side at 614 cm^{-1} , which corresponds to C–Cl stretching in the alkyl group. The strong intense peaks at 1382 cm^{-1} correspond to C–N stretch vibrations, as well as to the amide I bands of proteins in the leaf extract (Gurunathan et al. 2015). The strong bands at 1074 cm^{-1} are due to ether linkages and suggest the presence of flavanones adsorbed on the surface of metal nanoparticles (Shankar et al. 2004). The phenolic groups participating in ion replacement response are placed in the 1315–1037 and 1456–1600 cm^{-1} regions for the plant extract (Jeeva et al. 2014b). The very strong band at 1592 cm^{-1} is due to C=C stretching in the aromatic ring, confirming the presence of the aromatic group (Reddy et al. 2014). The silver nanoparticles of O–H stretching in carboxylic acids vibration is shifted from 3785 to 3881 cm^{-1} . The immediate reduction and capping of silver ion into silver nanoparticles in the present analysis might be due to flavanoids and proteins. The flavanoids present in the leaf extract are powerful reducing agents which may be suggestive of the formation of AgNPs by reduction of silver nitrate. The flavonoid compounds in the water extract of *M. pendans* might be actively involved and responsible for the reduction of Ag^+ to Ag^0 (Zuas et al. 2014). The involvement of water-soluble flavonoid in the reduction of metal ions using plant extracts is also evidenced from another study (Prabhu et al. 2010).

XRD studies

The nanoparticles synthesised in this method are characterized using powder XRD to confirm the particles as silver

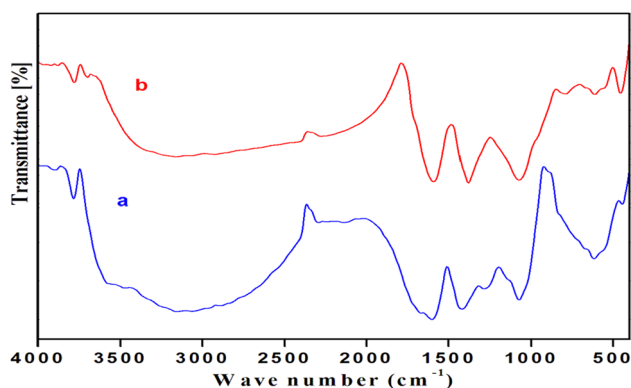


Fig. 5 FTIR spectra of *Pedalium murex* **a** before reaction and **b** after reaction with AgNO_3

and to know the structural information. Figure 6 shows the XRD pattern of silver nanoparticles.

The pattern clearly shows the main peaks at (2θ) 38.19, 44.37, 64.56 and 77.47 corresponding to the (111), (200), (220) and (311) planes, respectively. By comparing JCPDS (file no: 89-3722), the typical pattern of green-synthesized AgNPs is found to possess an fcc structure. The average crystalline size of the silver nanoparticles was estimated using (Eq. 1), the Debye–Scherrer’s equation (Ajitha et al. 2014):

$$D = 0.9\lambda/\beta \cos \theta. \quad (1)$$

By determining the width of (111) Bragg’s reflection, the estimated average size of the particle is 14 nm.

In addition, two unassigned peaks appeared at 32.25° and 46.21°. These peaks were weaker than those of silver. This may be due to the bioorganic compounds occurring on the surface of the AgNPs. Unpredicted crystalline structures (32.25° and 46.21°) are also present and might be due to the organic compounds in the leaf extract (Suvith and Philip 2014; Duraisamy et al. 2013). A similar result was observed by Kumar and Yadav (2009) and Jeeva et al. (2014b), who identified crystalline peaks (32.28°, 46.28°, 54.83°, 67.47° and 76.69°) which were also obvious in a lot of works in which the XRD pattern included the relevant 2° range. Appearances of these peaks are due to the presence of phytochemical compounds in the leaf extracts. The stronger planes indicate silver as a major constituent in the biosynthesis.

The average crystalline size, lattice parameter, cell volume and microstrain are shown in Table 1. The calculated lattice constant is in good agreement with the reported value and the sample exhibits smaller cell volumes. Earlier workers reported similar results for Ag nanoparticles (Gopinath et al. 2012; Basavegowda et al. 2014; Bindhu and Umadevi 2013).

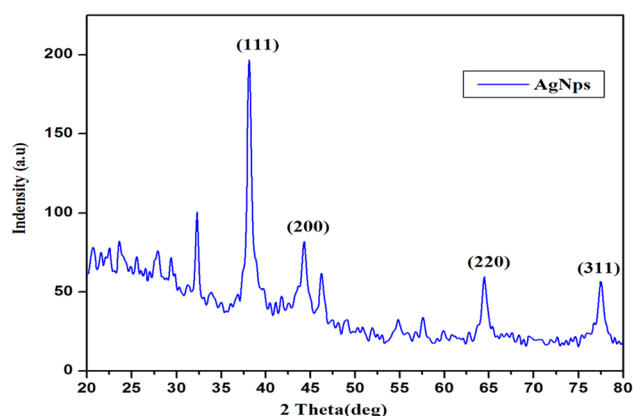


Fig. 6 XRD pattern of *Pedalium murex* extract synthesized silver nanoparticles

Table 1 The variation of crystalline size, lattice parameter, cell volume and microstrain value of biosynthesized nanoparticles

2θ	Orientation	Crystalline size (nm)	Lattice constant (\AA)	Cell volume (\AA^3)	Microstrain
38.11	(111)	18.32	4.0874	68.2875	0.00579
44.22	(200)	10.74	4.0940	68.6225	0.00861
64.45	(220)	12.05	4.0868	68.2574	0.00543
77.40	(311)	15.31	4.0856	68.2014	0.00361

FESEM analysis

The FESEM images of the silver nanoparticles are shown in Fig. 7. The surface morphology of silver nanoparticles showed even shape and spherical nature. In the present study, the histogram of the particle size ranges from 20 to 50 nm. Similar results were also reported for phyto-synthesised silver nanoparticles (Sathishkumar et al. 2012). This result strongly confirms that *Pedaliium murex* leaf extracts might act as a reducing and capping agent in the production of silver nanoparticles.

EDAX study

Figure 8 shows the energy dispersive spectrum of the synthesized nanoparticles, which suggests the presence of silver as the ingredient element. Metallic silver nanoparticles generally show a typically strong signal peak at 3 keV, due to surface plasmon resonance (Magudapatty et al. 2001; Kaviya et al. 2011; Das et al. 2013). Figure 8 shows the quantitative information of biosynthesized AgNPs. The presence of elements such as Ag, O, C, K, Cl, Ca and Na are shown in the inset of Fig. 8.

This is one of the advantages of nanoparticles synthesized using plant extracts over those synthesised using chemical methods. In the present investigation, the

synthesized silver nanoparticles show strong absorption in the range 2.5–4 keV. Similar results were reported earlier and the formation of silver nanoparticles was in the range 2–4 keV using *Artemisia nilagirica* leaf and *Artocarpus heterophyllus* seed extracts by Jagtap and Bapat (2013) and Vijaykumar et al. (2013).

TEM analysis of AgNPs

The shape and size of the resultant particles were elucidated with the help of TEM (Fig. 9). Aliquots of Ag nanoparticle solution were placed on a carbon-coated copper grid and allowed to dry under ambient conditions and TEM image were recorded. The TEM micrographs suggest that the sizes of the particles were around 50 nm. The particles were of spherical shape. The size measured by TEM analysis was lower than that measured by DLS analysis.

DLS and zeta potential

The DLS size distribution image of biosynthesized silver nanoparticles is shown in Fig. 10a. It is observed that the size distribution of AgNPs ranges from 10 to 150 nm. The calculated average particle size distribution of AgNPs is 73.14 nm. The broad spectrum of DLS analyzer confirms

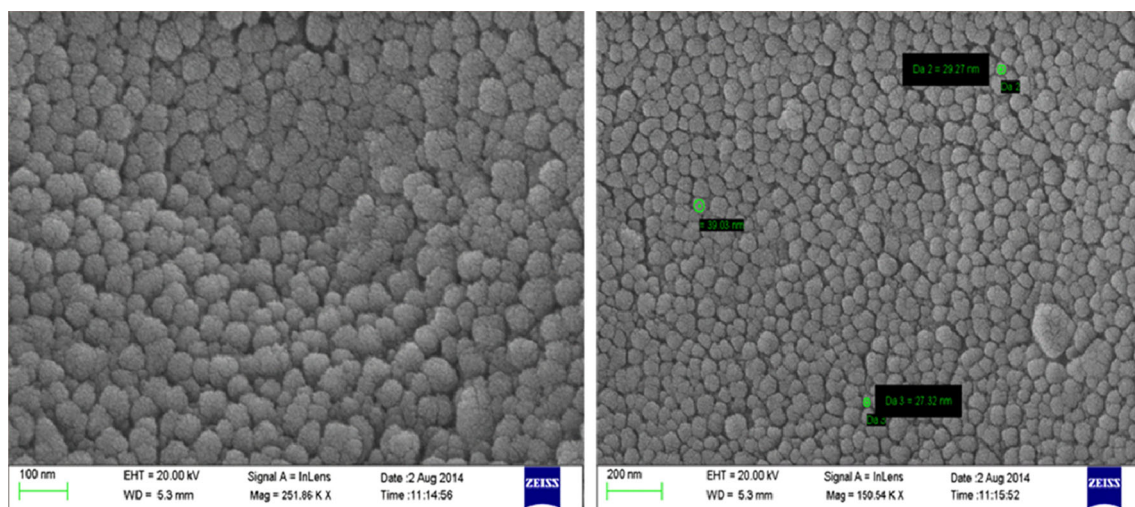
**Fig. 7** FE-scanning electron microscope image of silver nanoparticles synthesised using *Pedaliium murex* leaf extracts at different magnifications

Fig. 8 EDAX spectrum of synthesised AgNPs using *Pedaliium murex* leaf extract

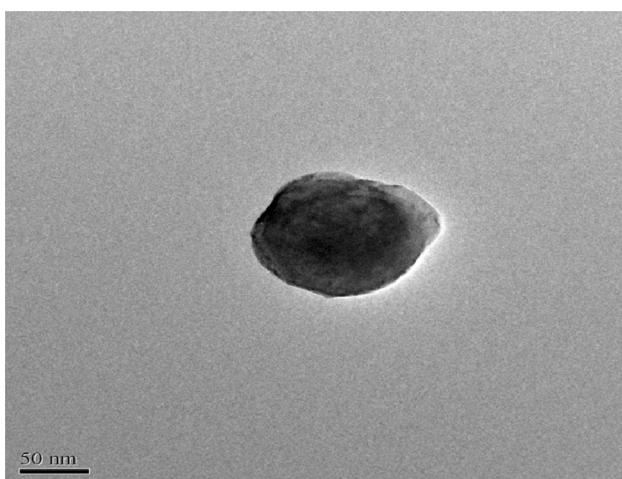
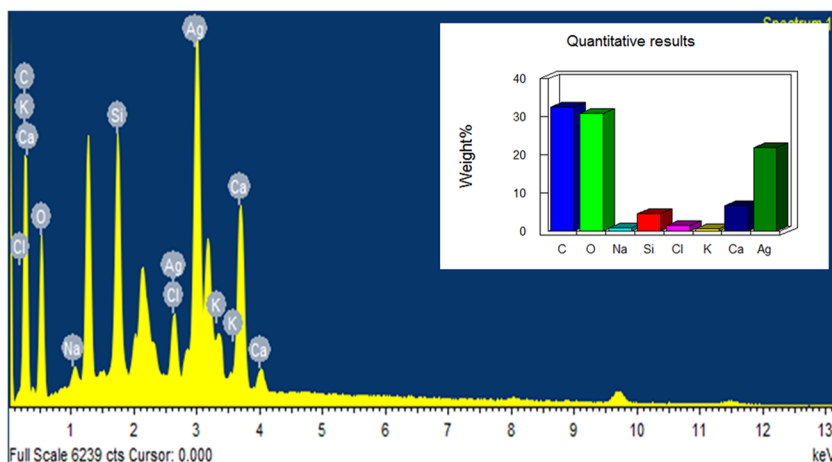


Fig. 9 TEM pictures of spherical silver nanoparticles

that the particle size is decreased when compared with the sharp SPR peak (424 nm) obtained in the UV–Vis spectra. In earlier reports, the average diameters of the particles were 53.2 nm. The zeta potential of the biosynthesised AgNPs was found as a sharp peak at -7.66 mV (Fig. 10b). It is suggested that the surface of the nanoparticles is negatively charged and dispersed in the medium. The negative value confirms the repulsion among the particles and proves that they are very stable.

Antimicrobial activity

In the present investigation, the antibacterial effect of prepared silver nanoparticles is studied on different types of bacteria such as *E. coli*, *K. pneumoniae*, *P. aeruginosa* (Gram negative) *M. flavus*, *B. subtilis*, *B. pumilus* and *S.*

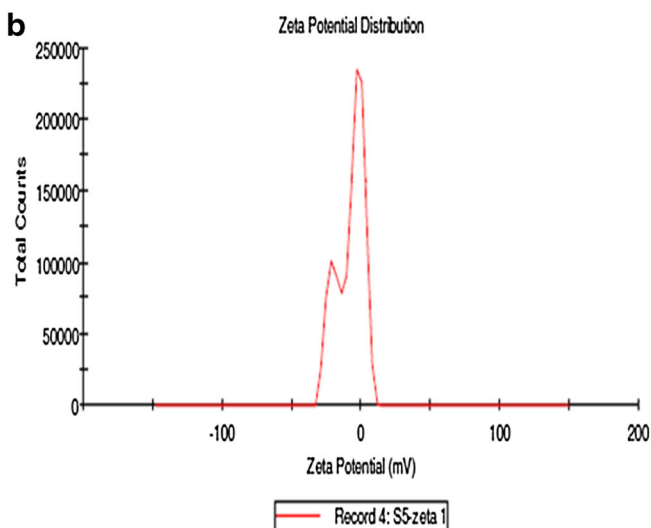
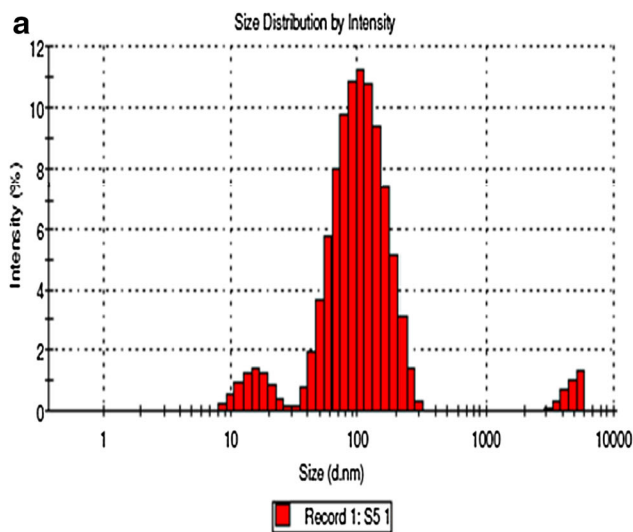


Fig. 10 DLS (a) and zeta potential (b) of AgNPs

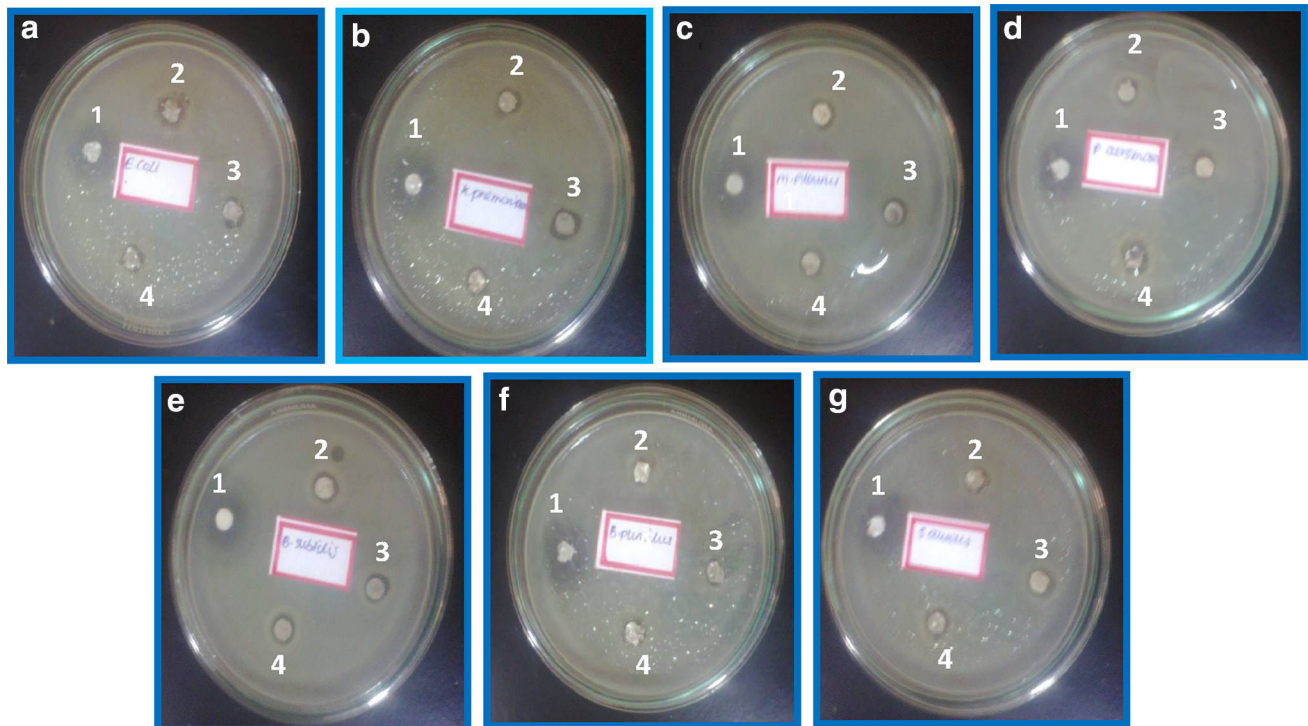


Fig. 11 Antibacterial activity of AgNPs against various bacterial strains [control (1), 5 µl/ml (2), 10 µl/ml (3), 15 µl/ml (4)]

Table 2 Antibacterial activity of the silver nanoparticles

Bacterium name	Zone of inhibition of Ag NPs (mm)			
	Control (ofloxacin) 2 mg/ml	5 µl/ml	10 µl/ml	15 µl/ml
<i>Escherichia coli</i>	17.5	9	9.5	10.5
<i>Klebsiella pneumoniae</i>	16.5	9	10	8.5
<i>Micrococcus flavus</i>	17.5	9.5	9.5	9
<i>Pseudomonas aeruginosa</i>	13	7.5	9	10.5
<i>Bacillus subtilis</i>	17.5	9.5	9.5	10
<i>Bacillus pumilus</i>	18	7.5	8	9.5
<i>Staphylococcus aureus</i>	17.5	8.5	9.5	9.5

aureus (Gram positive). The antibacterial activities of three different concentrations of AgNPs with seven microorganisms were studied. The zone of incubation around AgNPs individual bacterial culture is shown in Fig. 11. The numerical value of the inhibition zone and the control antibiotic ofloxacin are given in Table 2. Bankar et al. (2010) reported the antibacterial activity of AgNPs using *E. coli*, *E. aerogenes*, *Klebsiella* sp. and *Shigella* spp. In the present study, the synthesised AgNPs had the highest antibacterial activity against *E. coli* and *B. subtilis*, respectively. Lesser antibacterial activity of AgNPs is observed against *K. pneumoniae*, *M. flavus*, *P. aeruginosa*, *B. pumilus* and *S. aureus*, while increasing (5, 10, 15 µl/ml) the concentration of Ag nanoparticles. These bacterial

group incubations around the wall are due to the release of diffusible inhibitory compounds from silver nanoparticles. These biosynthesized nanoparticles are widely used in cancer therapy, wound healing, antimicrobial activity, water paints, cotton fabrics and textiles, etc. The green synthesis of AgNPs has also paved a better methodological approach in the medical field.

Conclusion

The green synthesis method is eco-friendly, of low cost and capable of producing AgNPs at room temperature. Here, *Pedalium murex* leaf extracts act as both reducing

and stabilizing agents. The AgNPs were characterized by UV–Vis, FTIR, XRD, DLS-zeta potential, FESEM, EDAX and TEM analysis. The UV–Vis spectral studies confirmed the surface plasmon resonance of green-synthesized silver nanoparticles. Biomolecules were responsible for reducing and capping of AgNPs, which were confirmed by FTIR measurements. Elemental analysis and particle stabilization were determined by EDAX and zeta potential techniques. FESEM studies revealed spherical and uniform-shaped silver nanoparticles with size in the range 20–50 nm. The XRD pattern showed fcc crystal structure. The average particle size was confirmed by TEM analysis. The biosynthesized AgNPs were found to have a pronounced antibacterial activity against *E. coli*, *K. pneumonia*, *M. flavus*, *P. aeruginosa*, *B. subtilis*, *B. pumilus* and *S. aureus*. In this present study, proteins and flavonoids in the *Pedaliium murex* leaf extract play an important role in the formation of silver nanoparticles.

Open Access This article is distributed under the terms of the Creative Commons Attribution 4.0 International License (<http://creativecommons.org/licenses/by/4.0/>), which permits unrestricted use, distribution, and reproduction in any medium, provided you give appropriate credit to the original author(s) and the source, provide a link to the Creative Commons license, and indicate if changes were made.

References

- Ajitha B, Ashok Kumar Reddy Y, Sreedhara Reddy P (2014) Biogenic nano-scale silver particles by *Tephrosia purpurea* leaf extract and their inborn antimicrobial activity. *Spectrochim Acta Part A* 121:164–172
- Bankar A, Joshi B, Kumar AM, Zinjarde S (2010) Banana peel extract mediated novel route for the synthesis of silver nanoparticles. *Coll Surf A Physicochem Eng Asp* 368:58–63
- Basavegowda N, Idhayadhulla A, Lee YR (2014) Preparation of Au and Ag nanoparticles using *Artemisia annua* and their in vitro antibacterial and tyrosinase inhibitory activities. *Mater Sci Eng C* 43:56–64
- Bindhu MR, Umadevi M (2013) Synthesis of monodispersed silver nanoparticles using *Hibiscus Cannabinus* leaf extract and its antimicrobial activity. *Spectrochim Acta Part A* 101:184–190
- Das J, Das MP, Velusamy P (2013) *Sesbania grandiflora* leaf extract mediated green synthesis of antibacterial silver nanoparticles against selected human pathogens. *Spectrochim Acta Part A* 104:265–270
- Dipankar C, Murugan S (2012) The green synthesis, characterization and evaluation of the biological activities of silver nanoparticles synthesized from *Iresine herbstii* leaf aqueous extracts. *Coll Surf B* 98:112–119
- Gopinath V, Mubarak Ali D, Priyadarshini S, Meera Priyadarshini N, Thajuddin N, Velusamy P (2012) Biosynthesis of silver nanoparticles from *Tribulus terrestris* and antimicrobial activity: a novel biological approach. *Coll Surf B* 96:69–74
- Gurunathan S, Jeong JK, Han JW, Zhang XF, Park JH, Kim JH (2015) Multidimensional effects of biologically synthesized silver nanoparticles in *Helicobacter pylori*, *Helicobacter felis*, and human lung (L132) and lung carcinoma A549 cells. *Nanoscale Res Lett* 10:35. doi:10.1186/s11671-015-0747-0
- Jagtap UB, Bapat VA (2013) Green synthesis of silver nanoparticles using *Artocarpus heterophyllus* Lam. seed extract and its antibacterial activity. *Ind Crops Prod* 46:132–137
- Jeeva K, Thiyagarajan M, Elangovan V, Geetha N, Venkatachalam P (2014a) *Caesalpinia coriaria* leaf extracts mediated biosynthesis of metallic silver nanoparticles and their antibacterial activity against clinically isolated pathogens. *Ind Crops Prod* 52:714–720
- Jeeva K, Thiyagarajan M, Elangovan V, Geetha N, Venkatachalam P (2014b) *Caesalpinia coriaria* leaf extracts mediated biosynthesis of metallic silver nanoparticles and their antibacterial activity against clinically isolated pathogens. *Ind Crops Prod* 52:714–720
- Jiang H, Manolache S, Lee Wong AC, Denes FS (2004) Plasma enhanced deposition of silver nanoparticles onto polymer and metal surfaces for the generation of antimicrobial characteristics. *J Appl Polym Sci* 93:1411–1422
- Jiang Zhiliang, Yuan Weien, Pan Hongcheng (2005) Luminescence effect of silver nanoparticle in water phase. *Spectrochim Acta Part A* 61:2488–2494
- Johnson I, Prabu HJ (2015) Green synthesis and characterization of silver nanoparticles by leaf extracts of *Cycas circinalis*, *Ficus amplissima*, *Commelina benghalensis* and *Lippia nodiflora*. *Int Nano Lett* 5:43–51
- Kalpana D, Lee YS (2013) Synthesis and characterization of bactericidal silver nanoparticles using cultural filtrate of simulated microgravity grown *Klebsiella pneumoniae*. *Enzyme Microb Technol* 52:151–156
- Kaviya S, Santhanalakshmi J, Viswanathan B, Muthumany J, Srinivasan K (2011) Biosynthesis of silver nanoparticles using *citrus sinensis* peel extract and its antibacterial activity. *Spectrochim Acta Part A* 79:594–598
- Kelly L, Coronado E, Zhao LL, Schatz GC (2003) The optical properties of metal nanoparticles: the influence of size, shape and dielectric environment. *J Phy Chem B* 107:668–677
- Khan Z, Hussain JI, Hashimi AA (2012) Shape-directing role of cetyltrimethylammonium bromide in the green synthesis of Ag-nanoparticles using neem (*Azadirachta indica*) leaf extract. *Coll Surf B* 95:229–234
- Kumar V, Yadav SK (2009) Plant mediated synthesis of silver and gold nanoparticles and their applications. *J Chem Technol Biotechnol* 84:151–157
- Lee KL, El-sayed MA (2006) Gold and silver nanoparticles in sensing and imaging: sensitivity of plasmon response to size, shape, and metal composition. *J Phy Chem B* 110:19220–19225
- Magudapatty P, Gangopadhyayans P, Panigrahi BK, Nair KGM, Dhara S (2001) Electrical transport studies of Ag nanoclusters embedded in glass matrix. *Phy B* 299:142–146
- Medda S, Hajra A, Dey U, Bose P, Mondal NK (2014) Biosynthesis of silver nanoparticles from *Aloe vera* leaf extract and antifungal activity against *Rhizopus* sp. and *Aspergillus* sp. *Appl Nanosci*. doi:10.1007/s13204-014-0387-1
- Mohamed MB, Volkov V, Link S, Sayed MAE (2000) The ‘lightning’ gold nanorods: fluorescence enhancement of over a million compared to the gold metal. *Chem Phy Lett* 317:517–523
- Niraimathi KL, Sudha V, Lavanya R, Brindha P (2013) Biosynthesis of silver nanoparticles using *Alternanthera sessilis* (Linn.) extract and their antimicrobial, antioxidant activities. *Coll Surf B* 102:288–291
- Njagi EC, Huang H, Stafford L, Genuino H, Galindo HM, Collins JB, Hoag GE, Suib SL (2011) Biosynthesis of iron and silver nanoparticles at room temperature using aqueous *Sorghum* bran extracts. *Langmuir* 27:264–271
- Patel DK, Laloo D, Kumar R, Hemalatha S (2011) *Pedaliium murex* Linn.: an overview of its phyto pharmacological aspects. *Asian Pac J Trop Med* 4(9):748–755

- Prabakar K, Sivalingam P, Mohamed Rabeek SI, Muthuselvam M, Devarajan N, Arjunan A, Karthick R, Suresh MM, Wembonyama JP (2013) Evaluation of antibacterial efficacy of phyto fabricated silver nanoparticles using *Mukia scabrella* (Musumusukkai) against drug resistance nosocomial gram negative bacterial pathogens. *Coll Surf B* 104:282–288
- Prabhu N, Raj DT, Yamuna GK, Ayisha SS, Joseph Puspha ID (2010) Synthesis of silver phyto nanoparticles and their anti-bacterial efficacy. *Dig J Nanomater Bios* 5:185–189
- Rai M, Gade A, Yadav A (2011) Biogenic nanoparticles: an introduction to what they are, how they are synthesized and their applications. In: Rai M, Duran N (eds) *Metal nanoparticles in microbiology*. Springer, Berlin, pp 1–16
- Rajashekar V, Upender Rao E, Srinivas P (2012) Biological activities and medicinal properties of Gokhru (*Pedalium murex* L.). *Asian Pac J Trop Biomed* 2(7):581–585
- Raveendran P, Fu J, Wallen SL (2003) Completely green synthesis and stabilization of metal nanoparticles. *J Am Chem Soc* 125:13940–13941
- Reddy NJ, Vali DN, Rani M, Rani SS (2014) Evaluation of antioxidant, antibacterial and cytotoxic effects of green synthesized silver nanoparticles by *Piper longum* fruit. *Mater Sci Eng C* 34:115–122
- Sathishkumar G, Gobinath C, Karpagam K, Hemamalini V, Premkumar K, Sivaramakrishnan S (2012) Phyto-synthesis of silver nano scale particles using *Morinda citrifolia* L. and its inhibitory activity against human pathogens. *Coll Surf B* 95:235–240
- Saxena A, Tripathi RM, Zafar F, Singh P (2012) Green synthesis of silver nanoparticles using aqueous solution of *Ficus benghalensis* leaf extract and characterization of their antibacterial activity. *Mater Lett* 67:91–94
- Shankar SS, Rai A, Absar Ahmad A, Sastry M (2004) Rapid synthesis of Au, Ag, and bimetallic Au core–Ag shell nanoparticles using neem (*Azadirachta indica*) leaf broth. *J Coll Interface Sci* 275:496–502
- Sharma VK, Yngard RA, Liny Y (2009) Silver nanoparticles; green synthesis and their antimicrobial activities. *Adv Coll Interface Sci* 145:83–96
- Singhal G, Bhavesh R, Kasariya K, Sharma AR, Singh RP (2011) Biosynthesis of silver nanoparticles using *Ocimum sanctum* (Tulsi) leaf extract and screening its antimicrobial activity. *J Nanopart Res* 13:2981–2988
- Suvith VS, Philip D (2014) Catalytic degradation of methylene blue using biosynthesized gold and silver nanoparticles. *Spectrochim Acta A Mol Biomol Spectrosc* 118:526–532
- Vigneshwaran N, Nachane RP, Balasubramanya RH, Varadarajan PV (2006) A novel one-pot ‘green’ synthesis of stable silver nanoparticles using soluble starch. *Carbohydr Res* 341:2012–2018
- Vijaykumar M, Priya K, Nancy FT, Noorlidaha A, Ahmed ABA (2013) Biosynthesis, characterization and anti-bacterial effect of plant-mediated silver nanoparticles using *Artemisia nilagirica*. *Ind Crops Prod* 41:235–240
- Yokohama K, Welchons DR (2007) The conjugation of amyloid beta protein on the gold colloidal nanoparticles surfaces. *Nanotechnology* 18:105101–105107
- Zargar M, Shameli S, Reza Najafi G, Farahani F (2014) Plant mediated green biosynthesis of silver nanoparticles using *Vitex negundo* L. extract. *J Ind Eng Chem* 20(6):4169–4175
- Zhang W, Qiao X, Chen J (2006) Synthesis and characterization of silver nanoparticles in AOT microemulsion system. *Chem Phy* 330:495–500
- Zuas O, Hamim N, Sampora Y (2014) Bio-synthesis of silver nanoparticles using water extract of *Myrmecodia pendans* (Sarang Semutplant). *Mater Lett* 123:156–159